

AN EXPLOSIVE POWDER ACCELERATOR HAVING A CYLINDRICAL RECESS FILLED WITH TUNGSTEN POWDER

S. K. Andilevko, G. S. Romanov,
and S. M. Usherenko

UDC 534.2

Numerical calculations are given on the parameters for a particle flow generated by an explosive accelerator having a cylindrical recess filled with powder.

Power-flow processing [1-3] involves a certain proportion of the particles penetrating to a depth $h \approx 10^4 d$ (d is initial particle size), which has been called superdeep penetration. The particle flow is produced by an explosive accelerator [4], in which there is a cylindrical charge having a recess in the lower part, which is filled with the powder. Here we perform calculations on it for a cylindrical recess filled with tungsten powder. The large-particle method [5, 6] is used.

Figure 1 shows the scheme (z is the symmetry axis), with the accelerator split up by a uniform net into cells with step $H_r = H_z$. The grid step and the time step were determined on the basis of criteria for computational stability [6], the geometry, and the performance of the computer (BÉSM-6, PC/AT-286). The hydrodynamic parameters (p , V , U , E , ρ) were determined in dimensionless form: $\bar{V} = V/D$, $\bar{U} = U/D$, $\bar{p} = p/\rho_e D^2$, $\bar{\rho} = \rho/\rho_e$, $\bar{E} = E/D^2$, $\bar{t} = Dt/L_c$, $\bar{z} = z/L_c$, $\bar{r} = r/L_c$, in which L_c is the accelerator length (along with the controlling support).

The boundary conditions for the acceleration were formulated by a standard method [6] involving the formation of a layer of fictitious cells, in which we determined the values for the quantities after passage through the boundary of the working region. Here:

a) along the symmetry axis ($r = 0$), the no-flow condition applies (the component of the velocity along r changes sign at the axis, while the other quantities are unaltered);

b) at the free end and the side surface ($z = 0$, $z = 1$, $r = 0.334$), one has the condition for flow into vacuum (the velocities do not alter on passage through the boundaries, and the density and pressure in the fictitious cell corresponded to the density of air and atmospheric pressure, 10^5 GPa);

c) at the surface of the control support (internal), the no-flow conditions also applied; and

d) the powder was separated from the explosive and the air by a chain of markers, whose displacement speeds were determined by interpolating the velocities from three adjacent

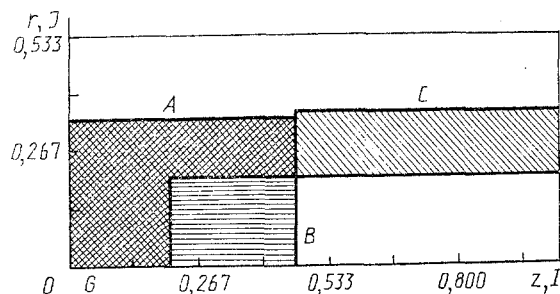


Fig. 1. Scheme for explosive accelerator: A) charge, B) cylindrical recess filled with powder, C) controlling support, G) electrical detonator.

Belorussian Powder Metallurgy Cooperative, Minsk. Translated from *Inzhenerno-Fizicheskii Zhurnal*, Vol. 61, No. 1, pp. 46-51, July, 1991. Original article submitted August 21, 1990.

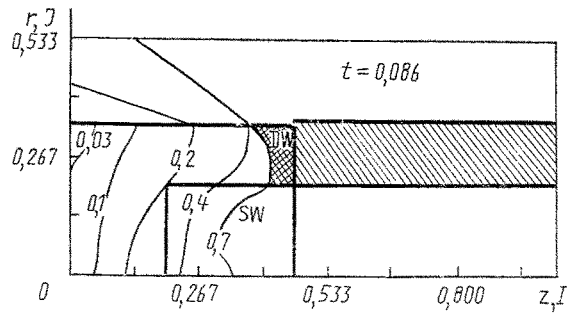
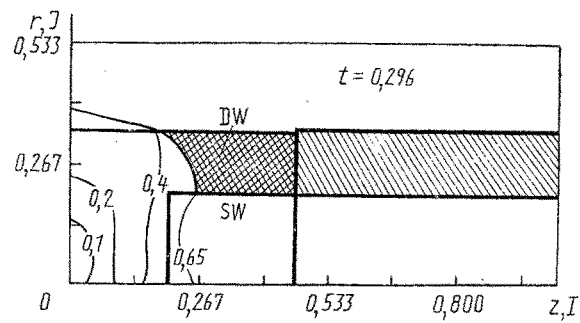


Fig. 2. Pressure isolines.

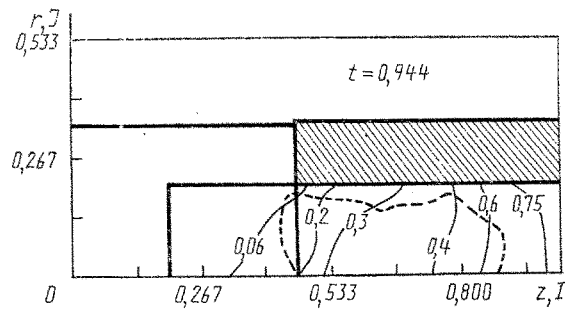
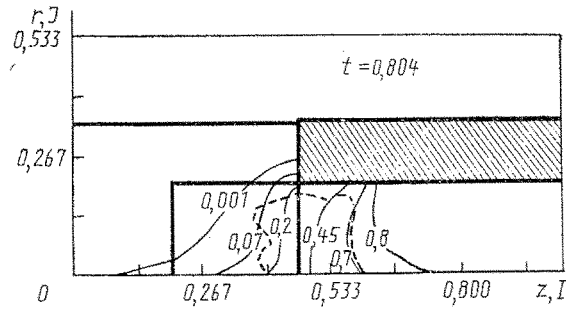


Fig. 3. Flow velocity isolines for accelerator with control support.

cells. The marker chain always remained continuous and was closed by the symmetry axis; the number of markers in a cell was 0 or 1.

The pressure in the material was determined from the equation of state, which for W powder was taken in the Tait form [7]:

$$p(\rho) = \begin{cases} 0, & \rho_{ip} \geq \rho \geq 0, \\ A[(\rho/\rho_{ip})^m - 1], & \rho \geq \rho_{ip}, \end{cases} \quad (1)$$

in which $A = 1.1 \cdot 10^6$ Pa, $m = 9.08$, $\rho_{ip} = 5.38 \cdot 10^3$ kg/m³. The equation of state for the explosive (ammonite) in regions A and G (Fig. 1) was taken in the [8] form. The space between the boundaries of the computing field and the square defined by the straight lines $z = 0.467$,

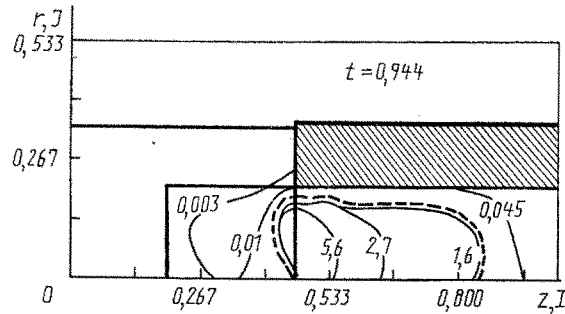
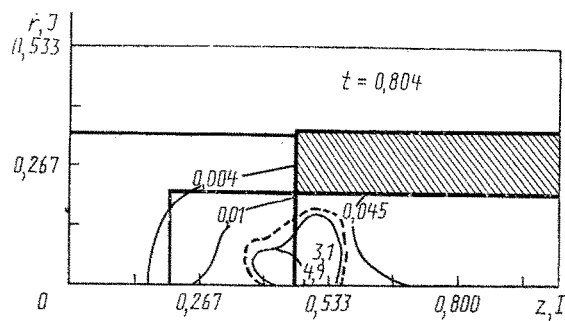


Fig. 4. Flow density isolines for accelerator with control support.

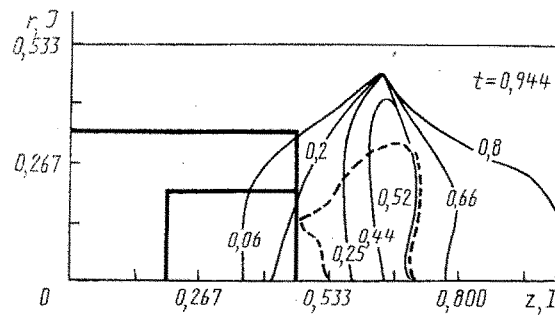
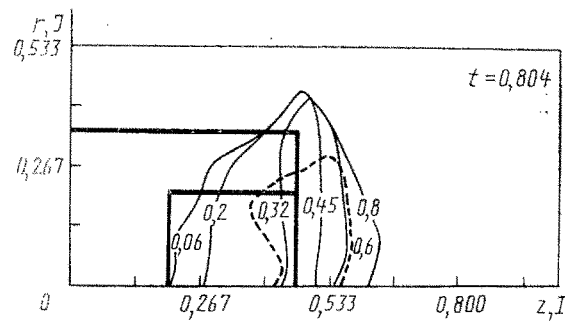


Fig. 5. Flow velocity isolines for an accelerator without control support.

$r = 0.2$ (or $r = 0.333$ in the absence of the controlling support) was filled with air with polytropic parameter $k = 1.4$.

The detonator G starts a detonation wave DW in the charge. The software implements this by increasing the internal energy in each cell in zone G (Fig. 1) by Q , which corresponds to the energy from that explosive [9]. Then at each time step Δt , $t_{n+1} = t_n + \Delta t$, the internal energy in each cell i, j containing the explosive was increased by Q if that cell was in the region

$$Dt_n \leq R = \sqrt{r^2 + z^2} \leq Dt_{n+1},$$

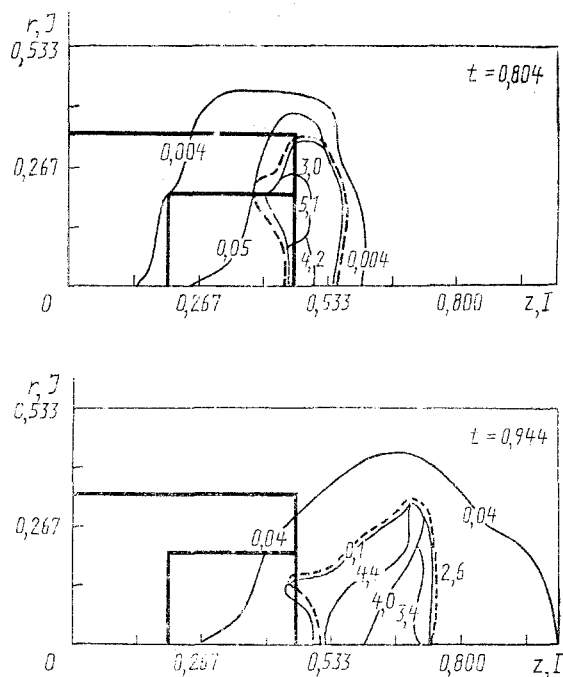


Fig. 6. Flow density isolines for accelerator without control support.

while the internal energy $E_{i,j}$ exceeded the activation energy E_a characteristic of that explosive [9].

When the DW was reached the surface of the powder recess (Fig. 2), a shock wave SW begins to propagate through the powder at $D_1 \approx 0.7$, and behind the front, the powder acquires a nonzero mass velocity. When the SW reaches the free surface ($z = 0.467$), a negative-positive wave propagates through the powder. The mass velocity of the powder behind that front increases. After the passage of that wave, the powder bunch motion is controlled by three factors: the inertia, the air resistance, and the impelling action of the detonation products.

Figures 3 and 4 show the velocity and flow density as functions of time. The variations in velocity U and density ρ at the level $z = 1$ can be approximated to 15-20% by exponentials:

$$U_f(t) = U_{af} \exp(-\alpha_1 t / \tau_0), \quad \rho_f(t) = \rho_{af} \exp(+\alpha_2 t / \tau_0), \quad (2)$$

in which $U_{af} \approx 2295$ m/sec, $\rho_{af} \approx 1107$ kg/m³, $\alpha_1 \approx 1.61$; $\alpha_2 \approx 0.92$, $D \approx 4495$ m/sec, and $\tau_0 \approx 7 \cdot 10^{-5}$ sec is the time from the first contact between the particle flow and the $z = 1$ surface to the instant when the last marker passes through it (total time for the flow motion through the $z = 1$ section), $0 \leq t \leq \tau_0$.

The section of the control support in Fig. 1 was established by calculations for an accelerator without it (the space C in Fig. 1 was filled with air). Figures 3 and 5 or Figs. 4 and 6 compare the results, where:

1. The geometrical outlines of the flow produced by the accelerator with control support (VU1) differ appreciably from those without it (VU2). In particular, the VU1 flow was extended along the axis and had a radius ≤ 0.15 and length ≈ 0.52 in dimensionless units. For VU2, the length was reduced to 0.16 with a radius of ~ 0.3 . The integral flow density for VU2 was 20-25% lower than that for VU1.

2. The mean speed of the flow from VU2 was 10-20% less than that from VU1, while the velocity of the head part was reduced by 20-25%, while the total time of motion was reduced by almost a factor two ($\tau_0 \approx 3.6 \cdot 10^{-5}$ sec).

The control support focuses the flow along the z axis because it prevents the flow from expanding sideways. The speed and density are increased somewhat. The integral characteristics for the VU2 flow can also be described approximately by (2) with $U_{af} \approx 1980$ m/sec, $\rho_{af} \approx 1003$ kg/m³, and $\alpha_1 \approx 1.54$, $\alpha_2 \approx 1.3$.

The mean velocities and densities were 1507 m/sec and 2752 kg/m³ for VU1 and 1108 m/sec and 2386 kg/m³ correspondingly for VU2.

NOTATION

z) symmetry axis; r) radial coordinate; ρ) density; p) pressure; U) mass velocity along z coordinate; V) mass velocity along z; E) energy; D) detonation speed; α) exponential coefficient; t) working time; τ) time segment. Subscripts denoting parameters: i) number of working cells along z; j) number of working cells along r; n) time step number; f) flow, af) approximation factor; a) activation; ip) initial powder parameters; e) explosive. A bar above a symbol denotes the dimensionless form.

LITERATURE CITED

1. K. I. Kozorezov, V. N. Maksimenko, and S. M. Usherenko, Selected Topics in Modern Mechanics, Part 1 [in Russian], Moscow (1981), pp. 115-119.
2. V. A. Shilkin, S. M. Usherenko, and S. K. Andilevko, Processing Materials at High Pressures: Coll. [in Russian], Kiev (1987), pp. 81-85.
3. L. V. Al'tshuler, S. K. Andilevko, G. S. Romanov, and S. M. Usherenko, Pis'ma Zh. Tekh. Fiz., 15, No. 5, 55-57 (1989).
4. S. K. Andilevko, G. S. Romanov, E. N. Sai, and S. M. Usherenko, Fiz. Goreniya Vzryva, 24, No. 7, 85-89 (1988).
5. O. M. Belotserkovskii and Yu. M. Davydov, The Large-Particle Method in Gas Dynamics: A Computational Experiment [in Russian], Moscow (1982).
6. O. M. Belotserkovskii, Simulation in Continuous-Medium Mechanics [in Russian], Moscow (1984).
7. A. A. Bakanova, I. P. Duduladov, and Yu. I. Sutulov, Zh. Prikl. Mat. Tekh. Fiz., No. 2, 116-122 (1974).
8. V. F. Kuropatenko, ChMMSS, 8, No. 6, 68-71 (1977).
9. F. A. Baum (ed.), Explosion Physics [in Russian], Moscow (1975).

MECHANISM AND FUNCTIONAL RELATIONS CHARACTERIZING THE INFLUENCE OF AMBIENT NOISE ON THE VITRIFICATION OF GLASS-FORMING SEMICONDUCTOR MELTS

M. I. Mar'yan and V. V. Khiminets

UDC 536.75

The influence of a random temperature field applied to a melt during the cooling process on the structure and properties of disordered materials is investigated. The functional relations established in the study are explained on the basis of the microinhomogeneous structure of the melts and the strongly nonlinear behavior of internal fluctuations in transition to the nonequilibrium state.

We have previously [1-4] proposed a synergetic approach to the study of vitrification processes during the cooling of melts of glass-forming semiconductors, based on allowance for the highly nonlinear dynamics of the internal fluctuations of the system (fluctuations of the fraction of atoms in fluidlike states and of the rms atomic displacements). These random fluctuations are insignificant under cooling conditions $q < q_c$ (q_c is the critical cooling velocity [1]), but are intensified outside the domain of stability of the equilibrium crystalline state ($q \geq q_c$), so that the mean fluctuation levels exhibit appreciable macroscopic variations [1-3]. However, the parameters describing a glass-forming melt dur-